Stresses in Soil-Bentonite Slurry Trench Cutoff Walls

Authors: Yu-Chao Li* (BEng, PhD, Associate Professor);
Peter John Cleall† (BEng, PhD, Senior Lecturer);
Yi-Duo Wen* (BEng, MEng candidate);
Yun-Min Chen* (BEng, MSc, PhD, Professor);
Qian Pan* (BEng, PhD candidate).

*MOE Key Laboratory of Soft Soils and Geoenvironmental Engineering, Department of Civil Engineering, Zhejiang University, Hangzhou 310058, China.
†Geoenvironmental Research Centre, Cardiff School of Engineering, Cardiff University, Cardiff, CF24 3AA, Wales, UK.

Submitting author:
Name: Yu-Chao Li
Contact address: MOE Key Laboratory of Soft Soils and Geoenvironmental Engineering, Department of Civil Engineering, Zhejiang University, Hangzhou 310058, China.
Telephone: +86-571-88208859
E-mail address: yuchao_li@hotmail.com.

Abstract: The long-term performance of soil-bentonite slurry trench cutoff walls is highly dependent on the hydraulic conductivity of the soil-bentonite backfill, which according to laboratory tests can decrease significantly as consolidation pressure increases due to corresponding reductions in void ratio. Consequently a reliable estimate of the hydraulic conductivity of backfill in the field requires proper calculation of effective stresses. A model is proposed to predict the steady-state horizontal and vertical effective stresses in the backfill after consolidation. The arching effect is considered via force equilibrium, and the lateral squeezing effect of inward displacement of the trench sidewalls is considered by assuming the cutoff wall is surrounded by soil which is represented by a Winkler idealization. The proposed model is applied to model a soil-bentonite slurry trench cutoff wall at Mayfield, New South Wales, Australia, and the predicted stress profile is in good agreement with that calculated from cone penetration tests data. Compared to those predicted by geostatics and other alternative models, the proposed method offers a significant improvement in the prediction of stress in SB slurry trench walls. The obtained stresses are then used to estimate the hydraulic conductivity in the backfill. It is found that the hydraulic conductivity is relatively high in the shallow region owing to the low state of effective stresses, which requires consideration in cutoff wall design, and decreases slightly with the depth in the deeper region. Finally a parametric study identifies the side wall friction and the modulus of horizontal subgrade reaction of surrounding soil as having the most significant impact on the estimated stresses.

Keywords: cut-off walls and barriers; permeability; stress analysis; trenches

1. Introduction

Soil-bentonite (SB) slurry trench cutoff walls are commonly constructed to contain subsurface contamination as part of a remediation strategy for contaminated sites. Typically a trench is excavated in the ground, with the trench being filled with slurry to maintain the trench stability. Then SB backfill is placed into the trench displacing the slurry to form a vertical barrier. The primary design criterion in SB cutoff wall design is an achievement of a low-permeability backfill barrier in the trench. Many laboratory tests show that hydraulic conductivity of SB decreases significantly as consolidation pressure increases due to corresponding reductions in void ratio (Evans 1994; Filz et al., 2001; Yeo et al., 2005). Accordingly, the *in-situ* stress state of SB backfills has a considerable effect on the hydraulic barrier performance of cutoff walls and subsequently a reliable estimate of the hydraulic conductivity of backfills in the field depends on the proper calculation of *in-situ* effective stress (Evans et al. 1995). The stress-state in the SB also has a critical influence on resistance to chemical attack and hydraulic fracturing of backfill (Filz 1996).

Early field and laboratory studies (McCandless & Bodocsi 1987; Bennert et al., 2005) indicate that the effective stress state in SB cutoff walls is much lower than that predicted by a geostatic approach where only the effective weight of the overlying backfill is considered. This finding has also been confirmed by various theoretical models (Evans et al., 1995; Filz, 1996; Ruffing et al., 2010). If the confining stress used in the laboratory tests is based on the vertical geostatic stress distribution the hydraulic conductivity of SB

backfill may be significantly underestimated, leading to a non-conservative design. Crucially, current design procedures of SB cutoff walls do not include consideration of the state of stress in backfill, and research efforts on SB cutoff walls has been largely limited to laboratory investigations, despite the need for an understanding of how the stress develops *in situ* (National Research Council, 2007; Ruffing et al., 2012).

The SB backfill consolidates under a vertical load from the weight of overlying backfill and a lateral squeezing load induced by the inward displacement of trench sidewalls. A closed-form solution based on an arching mechanism approach, conventionally applied to buried pipelines, was proposed by Evans et al. (1995) to calculate the steady-state vertical effective stresses in backfill of SB cutoff walls. This solution considers backfill sidewall friction, which reduces vertical stress in the backfill to magnitudes below that of the overburden pressure. However, in this approach the trench sidewalls are assumed to be rigid, which may result in an underestimation of the horizontal effective stress by ignoring strength gain in the backfill realized by inward movement of the trench sidewalls (Ruffing et al., 2010). An alternative "lateral squeezing" model had been proposed by Filz (1996) primarily accounting for the lateral squeezing mechanism due to the trench sidewalls' movement towards the trench centerline after backfill placement. Consistencies of lateral force and displacement at the interface between the backfill and the surrounding soil are considered. However, this model assumes that the sidewall frictional forces are capable of reducing the vertical stresses in the backfills (caused by overlying backfills) to negligible values, and so the obtained stresses are not dependent on the backfill overburden pressure. As noted by Filz (1996) this assumption is not valid

for wide and shallow trenches. The lateral squeezing model was modified by Ruffing et al. (2010) to incorporate consideration of the stress-dependent nature of SB backfill's compressibility. The primary limitations of the lateral squeezing models (Filz, 1996; Ruffing et al., 2010) are firstly that the ground adjacent to the trench is assumed to be in an at-rest condition prior to backfill compression, which may lead to errors in prediction of the steady-state stresses, and secondly that the relationship between lateral earth pressure (or lateral earth pressure coefficient) and trench sidewall movement, which the lateral squeezing models require, is not well established in the literature.

A model is proposed in this paper to predict the steady-state effective stresses in backfill of SB slurry trench cutoff walls. It combines the ideas of two existing models (Evans et al., 1995; Filz, 1996) considering both the arching and lateral squeezing mechanisms. The proposed model is then applied to model the stress distribution in a SB cutoff wall at Mayfield, New South Wales, Australia. The stress profile obtained by the proposed model is compared with that calculated from results of cone penetration tests given by Ruffing et al. (2015) as well as those predicted by geostatics, the arching model and the modified lateral squeezing (MLS) model. The hydraulic conductivity of the backfill with depth is estimated based on the obtained stresses. Finally, a parametric study is carried out to investigate the impacts of backfill/surrounding soil properties on the effective stresses in backfill.

2. Theory

A SB slurry trench cutoff wall, whose width and depth are B and L, respectively, within a soil medium is considered in this paper (see Fig. 1). It is assumed that the groundwater level is at the surface and that the SB backfill is fully saturated after placement (Evans et al., 1995; Filz, 1996; Ruffing et al., 2010). The longitudinal strain of backfill after the placement is assumed to be zero and so the geometry of the problem can be considered to be plane-strain. For simplicity, in the subsequent text the horizontal direction refers to the transverse direction. A two-dimensional coordinate system, whose positive direction is downward, is adopted, and the ground surface is chosen as the origin of z.

At the end of backfill placement, the self-weight of the SB is assumed to be fully carried by the pore water, that is, the pore water pressure $u=\gamma_w z+\gamma'_{sb} z$ in the backfill at the depth z (see Table 1), where γ_w is the unit weight of water and γ'_{sb} is the buoyant unit weight of SB backfill; the horizontal and vertical effective stresses in the backfill $\sigma'_h=\sigma'_v=0$; and the excess pore water pressure $u_e=\gamma'_{sb} z$. When the backfill is consolidated, u_e becomes zero; the pore water pressure decreases to hydrostatic pressure, that is, $u=\gamma_w z$; and the steady-state effective stresses σ'_h and σ'_v require determination.

The horizontal strain increment between the times of completion of backfill placement and backfill consolidation can be written as (Timoshenko, 1970),

$$\triangle\varepsilon_h=\frac{1-\mu^2}{E}\left(\triangle\sigma'_h-\frac{\mu}{1-\mu}\triangle\sigma'_v\right)=\frac{1-\mu^2}{E}\left(\sigma'_h-\frac{\mu}{1-\mu}\sigma'_v\right) \quad (1)$$

where $\triangle\varepsilon_h$, $\triangle\sigma'_h$ and $\triangle\sigma'_v$ are, respectively, the increments of horizontal strain, horizontal effective stress and vertical effective stress in the backfill between the times of completion of backfill placement and backfill consolidation; E and μ are the Young's modulus and Poisson's ratio of backfill, respectively.

The hydraulic conductivity of the surrounding soil is commonly greater than that of the SB backfill by at least one or two orders of magnitude. Consequently, the consolidation of the surrounding soil mass is assumed to be finished instantaneously, and the horizontal effective stress in the surrounding soil, $\sigma'_{h,s}$, can then be determined as follows,

$$\sigma'_{h,s} = \sigma_h - \gamma_w z \tag{2}$$

where σ_h is the horizontal total stress in backfill and its values at the end of backfill placement and the time of backfill consolidation completion are given in Table 1. According to the Winkler's idealization (Selvadurai, 1979), the surrounding soil is assumed to be equivalent to an infinite number of independent elastic springs (see Fig. 1). The deformation of the foundation at any point is directly proportional to the stress applied at that point. So the horizontal deformation of the trench sidewall between the time of SB backfilling completion and that of SB consolidation completion can be written as follows using Equ. (2),

$$\triangle y = \frac{\triangle\sigma'_{h,s}}{k} = \frac{\gamma'_{sb} z - \sigma'_h}{k} \tag{3}$$

where $\triangle y$ is the horizontal deformation of the trench side wall and $\triangle\sigma'_{h,s}$ is the horizontal effective stress increment in the surrounding soil; and k is the modulus of

horizontal subgrade reaction of the surrounding soil. Using Equ. (3), the horizontal strain increment can also be written as

$$\triangle\varepsilon_{\mathrm{h}} = \frac{2\triangle y}{B} = \frac{2}{Bk}\left(\gamma'_{\mathrm{sb}}\, z - \sigma'_{\mathrm{h}}\right) \tag{4}$$

The following relationship between σ'_{v} and σ'_{h} can be obtained by combining Equs. (1) and (4):

$$\sigma'_{\mathrm{v}} = D\sigma'_{\mathrm{h}} - A\gamma'_{\mathrm{sb}}\, z \tag{5}$$

where

$$A = \frac{2E}{\mu\left(1+\mu\right)Bk} \tag{6}$$

$$D = \frac{1-\mu}{\mu} + A \tag{7}$$

The vertical force equilibrium of a typical backfill element with a thickness dz (see Fig. 1) considering the "arching" effect (Handy, 1985) has the following expression, when the backfill is consolidated:

$$2\tau\mathrm{d}z + \left(u+\mathrm{d}u\right)B + \left(\sigma'_{\mathrm{v}} + \mathrm{d}\sigma'_{\mathrm{v}}\right)B = uB + \sigma'_{\mathrm{v}}\, B + \gamma_{\mathrm{sb}} B\mathrm{d}z \tag{8}$$

where γ_{sb} is the unit weight of the SB backfill; $B\mathrm{d}u = B\gamma_{\mathrm{w}}\mathrm{d}z$; and τ is the sidewall frictional stress at the backfill-surrounding soil interface (Evans et al., 1995; Ruffing et al., 2010) and is assumed to follow the Mohr-Coulomb strength criterion as follows,

$$\tau = c'_{\mathrm{inter}} + \sigma'_{\mathrm{h}} \tan\phi'_{\mathrm{inter}} \tag{9}$$

where c'_{inter} and ϕ'_{inter} are the cohesion and internal friction angle of the interface, respectively, and they are assumed to have the following relationships with those of SB backfill (Potyondy, 1961):

$$c'_{inter} = c'_{sb} / R \tag{10}$$

$$\tan\phi'_{inter} = \tan\phi'_{sb} / R \tag{11}$$

where c'_{sb} and ϕ'_{sb} are the cohesion and internal friction angle of the backfill, respectively; and R is the shear strength reduction factor. Equ. (8) can be re-written using as follows Equs. (5), (9)-(11),

$$\sigma'_h + \frac{BD}{2\tan\phi'_{inter}} \frac{d\sigma'_h}{dz} - \frac{B\gamma'_{sb}}{2\tan\phi'_{inter}} \left(1 + A - \frac{2c'_{inter}}{B\gamma'_{sb}}\right) = 0 \tag{12}$$

Equ. (12) is the governing equation in terms of the steady-state σ'_h. It is assumed that there is no surcharge load and so the steady-state horizontal effective stress at the top boundary of the cutoff wall can be written as

$$\sigma'_h = 0 \qquad \text{at} \quad z = 0 \tag{13}$$

Given σ'_h is known, σ'_v can be obtained using Equ. (5). The modulus of horizontal subgrade reaction k for soils has the following general form (Bowles, 1996):

$$k = A_s + B_s z^n \tag{14}$$

where A_s is constant; B_s is coefficient for depth variation; and n is exponent to give k the best fit. This non-linear relationship can be reduced to a linear form, which is commonly used in foundation engineering (Das, 1998), by taking a value of n=1 yielding:

$$k = n_h z \tag{15}$$

where n_h is the constant of modulus of horizontal subgrade reaction.

Equ. (12) can then be solved via a numerical method, with the finite element method used in this paper. It is noted that Equ. (12) has the following closed-form solution if k is assumed to be constant in depth:

$$\sigma'_h = \frac{B\gamma'_{sb}}{2\tan\phi'_{inter}}\left(1+A-\frac{2c'_{inter}}{B\gamma'_{sb}}\right)\left[1-\exp\left(-\frac{2\tan\phi'_{inter}}{BD}z\right)\right] \quad (16)$$

The squeezing effect due to inward displacements of trench sidewalls is considered in Equ. (16) via the coefficients A and D (as defined in Equs. (6) and (7)). This equation can be compared to the following solution of the arching model (Ruffing et al., 2010), which assumes the trench sidewalls are rigid,

$$\sigma'_h = K_{ob}\sigma'_v = \frac{B\gamma'_{sb}}{2\tan\phi'_{inter}}\left(1-\frac{2c'_{inter}}{B\gamma'_{sb}}\right)\left[1-\exp\left(-\frac{2K_{ob}\tan\phi'_{inter}}{B}z\right)\right] \quad (17)$$

where K_{ob} is the at-rest earth pressure coefficient of the backfill.

3. Validation

In order to assess the validity of the proposed model it has been applied to one of the only experimental datasets related to SB slurry trench cutoff walls where estimates of *in-situ* stress conditions are available. This case study relates to a SB cut-off wall constructed at the Mayfield site which is an area of land approximately 155 ha on the south bank of the Hunter River near Newcastle in New South Wales, Australia. Full details can be found in Jones et al. (2007); Ryan & Spaulding (2008) and Ruffing et al. (2015).

The most polluted part of the site, known as Area 1, was previously occupied by coke ovens, gas holders and other processes associated with steelmaking over a period of approximately 85 years. The geoenvironmental testing of samples from test pits showed that this site was high polluted by polycyclic aromatic hydrocarbons, Benzo(a)pyrene, Chromium and Lead. A SB slurry trench cutoff wall was designed and installed through a sand layer (which varied from 30 m to 50 m thick) to divert up gradient groundwater flows away from Area 1 and to stop the movement of contaminations towards the river. It is 1,510 m long, 0.8 m wide and has depths ranging from 25 m to 49 m. The excavated trench was backfilled with a SB mixture consisting of a blend of excavated soil, imported clay and bentonite slurry. A minimum fines (passing 75μm sieve) content of 20% in the backfill blend was checked daily with a target of achieving a permeability specification of less than 1×10^{-8} m/s (Jones et al 2007).

As part of the quality control program a series of cone penetration tests with pore pressure readings (CPTu) was performed producing 24 CPTu profiles through the full depth of the cutoff wall. In addition a vane test was performed to a depth of 18 m at one of the cone locations. The effective cone resistance method was selected from five potential methods (Powell & Lunne, 2005) by Ruffing et al. (2015) to predict the undrained shear strength (S_u) vs. depth, that is,

$$S_u = \frac{q_t - u_2}{N_{ke}} \tag{18}$$

where u_2 is pore pressure from CPTu data; N_{ke} is the theoretical cone factor with a value of N_{ke}=11.5 reported by Ruffing et al. (2015) based on the coupled CPTu and vane shear data; finally q_t is the corrected tip resistance via the following equation:

$$q_t = q_c + (1-a)u_2 \quad (19)$$

where q_c is raw tip resistance; and a is area ratio (reported as 0.73 by Ruffing et al. (2015) for these tests).

The major principal effective stress σ'_0 in the SB cutoff wall for this project (see Fig. 2) was calculated by Ruffing et al. (2015) from average S_u vs. depth of all 24 CPTu data sets, using a S_u / σ'_0 ratio of 0.22. This ratio was selected by Ruffing et al. (2015) based on a review of available values for normally consolidated soils. It is noted that the values of cone resistance were deleted if they were significantly larger than the surrounding data points (>300-500 kPa), as they may be caused by pieces of gravel suspended in the backfill. It can be seen in Fig. 2 that the major principal stress at a depth greater than 5 m is significantly less than that predicted by geostatics. This is consistent with the findings of early field and laboratory studies (McCandless & Bodocsi, 1987; Bennert et al., 2005).

Ruffing et al. (2015) assumed the horizontal effective stress was the major principal stress and controlled the backfill strength but recognized that the state of stress in SB slurry trench cutoff walls is not fully understood. As shown in Fig. 2, the horizontal effective stress predicted by Ruffing et al. (2015) using the arching model or the MLS model (with K_{ob}=0.5) is significantly less than the major principal stress calculated from the CPTu data. This is likely the result of only one of the arching and lateral squeezing effects being considered by each of these two models.

The proposed method is adopted to predict the effective stresses in the SB slurry trench cutoff wall installed at Mayfield. The values used for the geometry and material properties are listed in Table 2. The Poisson's ratio used for the backfill is based on data reported by Baxter (2000) for soil-bentonite backfills. The linear relationship between k and depth (Das, 1998) is used with the average value of n_h for submerged medium dense sand and dense sand (Das, 1998; DHURDZP, 2014) according to the geotechnical condition of the site (Jones et al., 2007). The shear strength of the backfill-surrounding soil interface is relatively low as a bentonite filter cake forms between backfill and surrounding soil during the construction of slurry trench cutoff walls, according to the findings of Lam et al (2014). Based on this, the shear strength reduction factor R is selected from the range between 0.10 and 0.20 via calibration using the major principal stress calculated from the CPTu data. It is recognized that direct measurement of R would reduce uncertainty related to this parameter; such measurements could be obtained following the approach reported by Lam et al (2014). The sensitivity of the model to this parameter is explored in the subsequent parametric study. The obtained vertical effective stress, which is greater than the horizontal one and assumed to be the major principal stress following the discussion of Ruffing et al. (2015), by the proposed method is in good agreement with that calculated from the CPTu data (see Fig. 2). Compared to those predicted by the arching model and the MLS model, the proposed model offers a significant improvement in the prediction of stress in SB slurry trench walls. This results from the proposed method considering the combined effects of arching and lateral squeezing.

The hydraulic conductivity of backfill (k_b) with depth can be estimated with the obtained stresses via consideration of changes in void ratio. Large strain consolidation models are available (e.g. Fox et al. (2014)) that relate the change in hydraulic conductivity to changes in void ratio through the compression curve; alternatively these relationships can be determined experimentally. As the relationship between the hydraulic conductivity and the effective consolidation stress is not available for the backfill material used in the Mayfield project, the following relationships for a sand-bentonite containing 5% dry bentonite tested by Yeo et al. (2005) are used to illustrate the potential impact:

$$e = 1.25 - 0.21\log\left(\frac{\sigma'(\text{kPa})}{5}\right) \tag{20}$$

$$k_b\,(\text{cm/s}) = 1.5\times10^{-7}\times10^{\frac{e-1.25}{0.22}} \tag{21}$$

where σ' is effective consolidation stress. As the consolidometer imposes one-dimensional loading conditions on the specimens the void ratio of the soil-bentonite is controlled by mean consolidation stress, rather than major principal consolidation stress (Adams et al., 1997). Consequently, the effective stresses obtained by the proposed model are converted to the equivalent vertical effective stress that would produce the same void ratio in one-dimensional compression condition following Filz et al. (2001):

$$\bar{\sigma}' = \frac{3\sigma'_{\text{mean}}}{1+2K_{\text{ob}}} \tag{22}$$

where $\bar{\sigma}'$ is the equivalent vertical effective stress; σ'_{mean} is the mean effective stress in backfill; and K_{ob} is assumed to be $\mu/(1-\mu)$ for the consolidometer tests. $\bar{\sigma}'$ can be re-written as the following express for the plane-strain problem considered in this paper:

$$\bar{\sigma}' = (1-\mu)(\sigma'_v + \sigma'_h) \tag{23}$$

Fig. 3 shows the estimated hydraulic conductivity profile based on the effective stresses obtained by the proposed model. In the shallow region ($z \leq 2.5$ m), k_b is relatively high owing to the low state of effective stresses (see Fig. 2); it then decreases with depth as effective stresses increase. In the deep region ($z > 5.0$ m), the estimated hydraulic conductivity decreases slightly with the depth as a result of the relatively constant value of the mean effective stress, and reaches a value of $\sim 1 \times 10^{-10}$ m/s at the depth of 30 m. According to the test results of Yeo et al. (2005), $k_b \leq 10^{-9}$ m/s can be achieved for the backfill containing only low-plasticity clay and the backfill consisting of clean, coarse-grained materials with a significant amount of dry bentonite if the effective consolidation stress $\sigma' \geq 10$ kPa. Consequently the hydraulic conductivity specification can be achieved at this site if the sand-bentonite reported by Yeo et al. (2005) is assumed to be used. The estimated hydraulic conductivity profile based on the geostatic stress is also shown in Fig. 3. It can be found that whilst the geostatic approach gives a good prediction in the shallow region ($z < 5.0$ m), it underestimates the hydraulic conductivity in the deep region ($z > 5.0$ m), which may lead to a non-conservative design.

4. Parametric study

In this section, the proposed model is applied to investigate the impacts of backfill/surrounding soil properties on the steady-state effective stresses in backfill.

Finally a discussion on the closed-form solution to the case with a constant k assumption is made.

The parameter values used to define trench geometry and material properties in the following investigations are listed in Table 3. In the table the values ahead of the brackets represent a base case scenario and those in the brackets define a range of values used to investigate the impact of the corresponding parameter. For the base case scenario, the width of the trench is 0.6 m; the depth of the trench is 30.0 m (the results obtained are also applicable to scenarios where L<30 m); the values for the properties of the SB backfill are based on Ruffing et al. (2010); the constant of modulus of horizontal subgrade reaction submerged medium sand (Das, 1998) is used for the surrounding soil (that is, n_h=4.8 MN/m^4); and the value for the shear strength reduction factor for the backfill-surrounding soil interface (that is, R=0.12) is based on the Mayfield case presented in the validation section.

The lateral squeezing effect of inward displacements of the trench sidewalls on the backfill is investigated via consideration of various values of n_h, in particular values of 1.2 MN/m^4, 4.8 MN/m^4 and 10.6 MN/m^4, which correspond to submerged loose, medium and dense sands, respectively (Das, 1998), are used. These values are based on those recommended for the design of retaining structures for foundation excavations (DHURDZP, 2014). As shown in Fig. 4(a) the horizontal effective stress, σ'_h, decreases due to less lateral squeezing effect as n_h increases. The effective stresses for the scenario in a dense sand formation are close to those for that in a medium sand formation, but they

are significantly different to those in a loose sand formation, which has a greater lateral squeezing force due to deformation of the sidewalls.

The vertical effective stress, σ'_v, predicted by the arching model (Ruffing et al., 2010), which assumes no lateral deformation of sidewalls, increases and tends towards $\frac{B\gamma'_{sb}}{2K_{ob}\tan\phi'_{inter}}\left(1-\frac{2c'_{inter}}{B\gamma'_{sb}}\right)$ as the depth increases (see Equ. (16)), that is, the weight of backfill tends to be taken by the sidewall friction with only a small increment in vertical effective stress with depth in the deeper regions. However, it is noted that, for the scenario in a loose sand formation, the vertical effective stress decreases as the depth increases when z>15 m due to higher horizontal effective stress induced by the lateral squeezing effect, which is considered in the proposed method.

The constrained modulus of the SB backfill M is in the range between 500 kPa to 1600 kPa based on a series of one-dimensional consolidation test tests for sand-bentonite with dry bentonite contents of 4 and 5 % (Yeo et al., 2005) and for SB backfill collected from a cutoff wall site in eastern Pennsylvania (Ruffing et al., 2010). The Young's modulus E of the backfill has the following relationship with M, according to elasticity theory:

$$E=\frac{(1+\mu)(1-2\mu)}{1-\mu}M \tag{24}$$

Three cases with E=312 kPa, 654 kPa and 997 kPa are considered for M=500 kPa, 1050 kPa and 1600 kPa, respectively. As shown in Fig. 4(b), compared to the use of E=654 kPa, the relative differences in σ'_h and σ'_v by using E=312 kPa are 4.7% and 0.1% respectively, and are 4.4% and 0.3% respectively by using E=997 kPa, at z=15 m.

Consequently it can be concluded that, Young's modulus of SB backfill does not have a major impact on the steady-state effective stresses in backfill and the use of a constant Young's modulus will not lead to appreciable errors.

The arching effect due to the trench sidewall friction is highly dependent on the shear strength reduction factor R, as shown in Fig. 4(c), which illustrates effective stress profiles for three cases with varied values of R (specified based on the Newcastle case modeled previously). The values of vertical effective stress for the cases with R=0.2, and 0.3 are 55.2% and 33.9%, respectively, of that for R=0.1, and those of horizontal effective stress are 60.1% and 41.2%, respectively.

A comparison between the results obtained by the numerical method which considers a linear increase of k with depth and those by the closed-form solution where the modulus of horizontal subgrade reaction k is assumed to be constant in depth is shown in Fig. 5. The k used for the closed-form solution is an average value throughout the domain of the cutoff wall (that is, $k=n_h L/2$). For the scenario in a loose sand formation, vertical effective stress is significantly underestimated by the closed-form solution, particularly in the deep region. This underestimation is because a higher sidewall friction is calculated by the closed-form solution due to greater lateral squeezing effects which result from a lower value of k being used in this region. The vertical effective stress calculated by the closed-form solution is 81.4% and 55.2% of that obtained by the numerical method at z=15 m and z=30 m, respectively. However, the closed-form solution gives a relatively

good prediction for the scenario in medium or dense sand formation, which as noted by Filz (1996), is not dominated by the lateral compression mechanism.

4. Conclusions

A model accounting for both arching and lateral squeezing effects has been proposed to predict the steady-state effective stresses in cutoff wall backfill. The proposed model was then applied to a SB slurry trench cutoff wall at Mayfield, New South Wales, Australia, and the predicted stress profile was found to be in good agreement with that calculated from CPTu data, provided an appropriate value of shear strength reduction factor is applied to the backfill. Compared with the stresses predicted by geostatics, the arching model and the MLS model, the proposed method offers a significant improvement in the prediction of stress in SB slurry trench walls. The obtained stresses can be used to estimate the hydraulic conductivity in the backfill. It was found that the hydraulic conductivity is relatively high in the shallow region owing to the low state of effective stresses, which requires consideration in cutoff wall design, and decreases slightly with the depth in the deeper regions. A parametric study found that: (1) the arching effect on the stresses in backfill is highly dependent on the sidewall friction, and laboratory tests on the shear strength of backfill-surrounding soil interface are required to get the value of R; (2) the modulus of the backfill does not have a significant impact on the effective stresses in backfill, compared to the modulus of horizontal subgrade reaction of surrounding soil; and (3) the closed-form solution significantly underestimates the stress

in the deep portion for the case in a loose sand formation; but it gives a relatively good prediction for the case in medium or dense sand formation.

Acknowledgement

The financial support received from the National Natural Science Foundation of China (NSFC) via Grant No. 51378465 and from the National High Technology Research and Development Program of China (863 Program) via Grant No. 2012AA062601 are gratefully acknowledged. The authors also wish to express their gratitude to Prof. Jeffrey C. Evans, Bucknell University for providing the data of the Mayfield case history.

List of Symbols

a	area ration of CPTu
c_k	change of hydraulic conductivity index
c'_{inter}	cohesion of backfill-surrounding soil interface
c'_{sb}	cohesion of SB backfill
k	modulus of horizontal subgrade reaction
k_b	hydraulic conductivity of SB backfill
k_{b0}	hydraulic conductivity at σ'_0
n	exponent to give modulus of horizontal subgrade reaction the best fit
n_h	constant of modulus of horizontal subgrade reaction
q_c	raw tip resistance of CPTu
q_t	corrected tip resistance of CPTu
u	pore water pressure
u_2	pore pressure read from CPTu
u_e	excess pore water pressure
y	Distance
z	Depth
A	Coefficient
A_s	constant of horizontal subgrade reaction

B	width of SB slurry trench cutoff wall
B_s	coefficient of horizontal subgrade reaction for depth variation
D	Coefficient
E	Young's modulus of SB backfill
K_{ob}	at-rest earth pressure coefficient of SB backfill
L	depth of SB slurry trench cutoff wall
N_{ke}	theoretical cone factor of CPTu
R	shear strength reduction factor
S_u	undrained shear strength of SB backfill
γ_w	unit weight of water
γ_{sb}	unit weight of SB backfill
γ'_{sb}	buoyant unit weight of SB backfill
μ	Poisson's ratio of SB backfill
σ_h	horizontal total stress in backfill
σ'	effective consolidation stress
σ'_0	major principal effective stress
σ'_h	horizontal effective stress in backfill
$\sigma'_{h,s}$	horizontal effective stress in surrounding soil
σ'_{mean}	mean effective stress
ϕ'_{sb}	internal friction angle of SB backfill
σ'_v	vertical effective stress in backfill
$\bar{\sigma}'$	equivalent vertical effective stress
τ	sidewall frictional stress at backfill-surrounding soil interface
ϕ'_{inter}	internal friction angle of backfill-surrounding soil interface

References

Adams, T., Baxter, D., Boyer, R., Britton, J., Henry, L., Heslin, G., and Filz, G. (1997). The Mechanical and Hydraulic Behavior of Soil-Bentonite Cutoff Walls, Progress Report No. 2. Virginia Polytechnic Institute and State University, Blacksburg, VA.

Baxter, D. Y. (2000). *Mechanical Behavior of Soil-bentonite Cutoff Walls*. Ph.D. Thesis, Virginia Polytechnic Institute and State University.

Bennert, T. A., Maher, A., and Jafari, F. (2005). Piezocone evaluation of a shallow soil-bentonite slurry wall. *Geo-Frontiers 2005*, GSP, ASCE, 1-14.

Bowles, J. E. (1996). *Foundation Analysis and Design*, McGraw-Hill Companies, Inc., New York.

Das, B. M. (1998). *Principles of Foundation Engineering*, Brooks/Cole Publishing Company, Pracific Grove, California, USA.

Department of Housing and Urban-Rural Development of Zhejiang Province (DHURDZP) (2014). Technical Specification for Building Foundation Excavation Engineering. Zhejiang Gongshan University Press, Hangzhou.

Evans, J. C. (1994). Hydraulic conductivity of vertical cutoff walls evans. *Hydraulic Conductivity and Waste Containment Transport in Soil*, ASTM, Philadelphia, 79-94.

Evans, J. C., Costa, M. J., and Cooley, B. (1995). The state-of-stress in soil-bentonite slurry trench cutoff walls. *Geoenvironment 2000: Characterization, Containment, Remediation, and Performance in Environmental Geotechnics*, ASCE, Geotechnical Specialty Publication, New York, NY, 1173-1191.

Filz, G. M. (1996). Consolidation stresses in soil-bentonite backfilled trenches. *The 2nd International Congress on Environmental Geotechnics*, Balkema, Rotterdam, 497-502.

Filz, G. M., Henry, L. B., Heslin, G. M., and Davidson, R. R. (2001). Determining hydraulic conductivity of soil-bentonite using the API filter press. *Geotechnical Testing Journal*, 24, No. 1, 61-71.

Fox, P. J., Pu, H. F., and Berles, J. D. (2014). CS3: Large Strain Consolidation Model for Layered Soils. *Journal of Geotechnical and Geoenvironmental Engineering*, 140, No. 8, 04014041-1-13.

Handy, R. L. (1985). The arch in soil arching. *Journal of Geotechnical Engineering-ASCE*, 111, No. 3, 302-318.

Jones, S., Spaulding, C., and Symth, P. (2007). Design and construction of a deep soil-bentonite groundwater barrier wall at Newcastle, Australia. *10th Australian New Zealand Conference on Geomechanics Common Ground*.

Lam, C., Jefferis, S. A., and Martin, C. M. (2014). Effects of polymer and bentonite support fluids on concrete-sand interface shear strength. *Géotechnique*, 64, No. 1, 28-39.

McCandless, R., and Bodocsi, A. (1987). Investigation of slurry cutoff wall design and construction methods for containing hazardous wastes. U.S. Environmental Protection Agency, Washington, D.C.

National Research Council (2007). *Assessment of the performance of engineered waste containment barriers*, National Academies Press, Washington, D.C.

Potyondy, J. G. (1961). Skin friction between various soils and construction materials *Géotechnique*, 11, No. 4, 339-353

Powell, J., and Lunne, T. (2005). Use of CPT data in clays/fine grained soils. *Studia Geotechnica et Mechanica*, 27, No. 3-4, 53-63.

Ruffing, D. G., Evans, J. C., and Malusis, M. A. (2010). Prediction of earth pressures in soil-bentonite cutoff walls. *GeoFlorida*, 2416-2425.

Ruffing, D. G., Evans, J. C., and Malusis, M. A. (2012). Long term in situ measurements of the volumetric water content in a soil-bentonite slurry trench cutoff wall. *GeoCongress 2012: State of the Art and Practice in Geotechnical Engineering*, 3429-3436.

Ruffing, D. G., Evans, J. C., and Ryan, C. R. Strength and stress estimation in soil bentonite slurry trench cutoff walls using cone penetration test data. *Proc., Proceedings of The International Foundations Congress and Equipment Expo 2015*.

Ryan, C. R., and Spaulding, C. A. (2008). Strength and permeability of a deep soil bentonite slurry wall. *GeoCongress 2008: Geotechnics of Waste Management and Remediation*, ASCE, 644-651.

Selvadurai, A. P. S. (1979). *Elastic Analysis of Soil-Foundation Interaction*, Elsevier Scientific Pub. Co., New York.

Timoshenko, S. (1970). *Theory of Elasticity*, McGraw-Hill Publishing Company, New York.

Yeo, S. S., Shackelford, C. D., and Evans, J. C. (2005). Consolidation and hydraulic conductivity of nine model soil-bentonite backfills. *Journal of Geotechnical and Geoenvironmental Engineering, ASCE*, 131, No. 10, 1189-1198.

List of Table and Figure Captions

Table 1. Pore pressure and horizontal stress in SB backfill at depth of *z*.

Table 2. Geometric and material properties for Mayfield site analysis.

Table 3. Geometric and material properties in parametric study.

Fig. 1. Diagram of a SB cutoff wall in Winkler foundation (not in scale).

Fig. 2. Predicted effective stress in soil-bentonite slurry trench cutoff wall of Mayfield site.

Fig. 3. Estimated hydraulic conductivity profiles based on effective stresses for soil-bentonite slurry trench cutoff wall of Mayfield site.

Fig. 4. Stress profiles obtained in parametric study.

Fig. 5. Stress profiles for varied functions of the modulus of horizontal subgrade reaction of surrounding soil.

Table 1. Pore water pressure and stress in SB backfill at depth of z.

Pore water pressure or stress in backfill at depth of z	Corresponding time	
	Backfill is placed	Backfill is consolidated
u_e	$\gamma'_{sb} z$	0
u	$\gamma_{sb} z$	$\gamma_w z$
σ'_h	0	to be determined
σ'_v	0	to be determined
σ_h	$\gamma_{sb} z$	$\gamma_w z + \sigma'_h$

Table 2. Geometric and material properties for Mayfield site analysis.

Parameter	Value	Unit
B	0.8*	m
γ'_{sb}	9.3[#]	kN/m^3
E	654[†]	kPa
μ	0.35	/
c'_{sb}	0.0[†]	kPa
ϕ'_{sb}	30.0[†]	°
n_h	7.7	MN/m^4
R	0.12	/

*: Jones et al. (2007); [#]: Ryan & Spaulding (2008); [†]: Ruffing et al. (2010).

Table 3. Geometric and material properties in parametric study.

Parameter	Value	Unit
B	0.6	m
L	30.0	m
γ'_{sb}	9.7*	kN/m^3
E	654 (312, 997)*	kPa
μ	0.35	/
c'_{sb}	0.0*	kPa
ϕ'_{sb}	30.0*	°
n_h	4.8 (1.2, 10.6)[#]	MN/m^4
R	0.12 (0.1, 0.2, 0.3)	/

*: from Ruffing et al. (2010); [#]: from Das (1998).

Figure 1

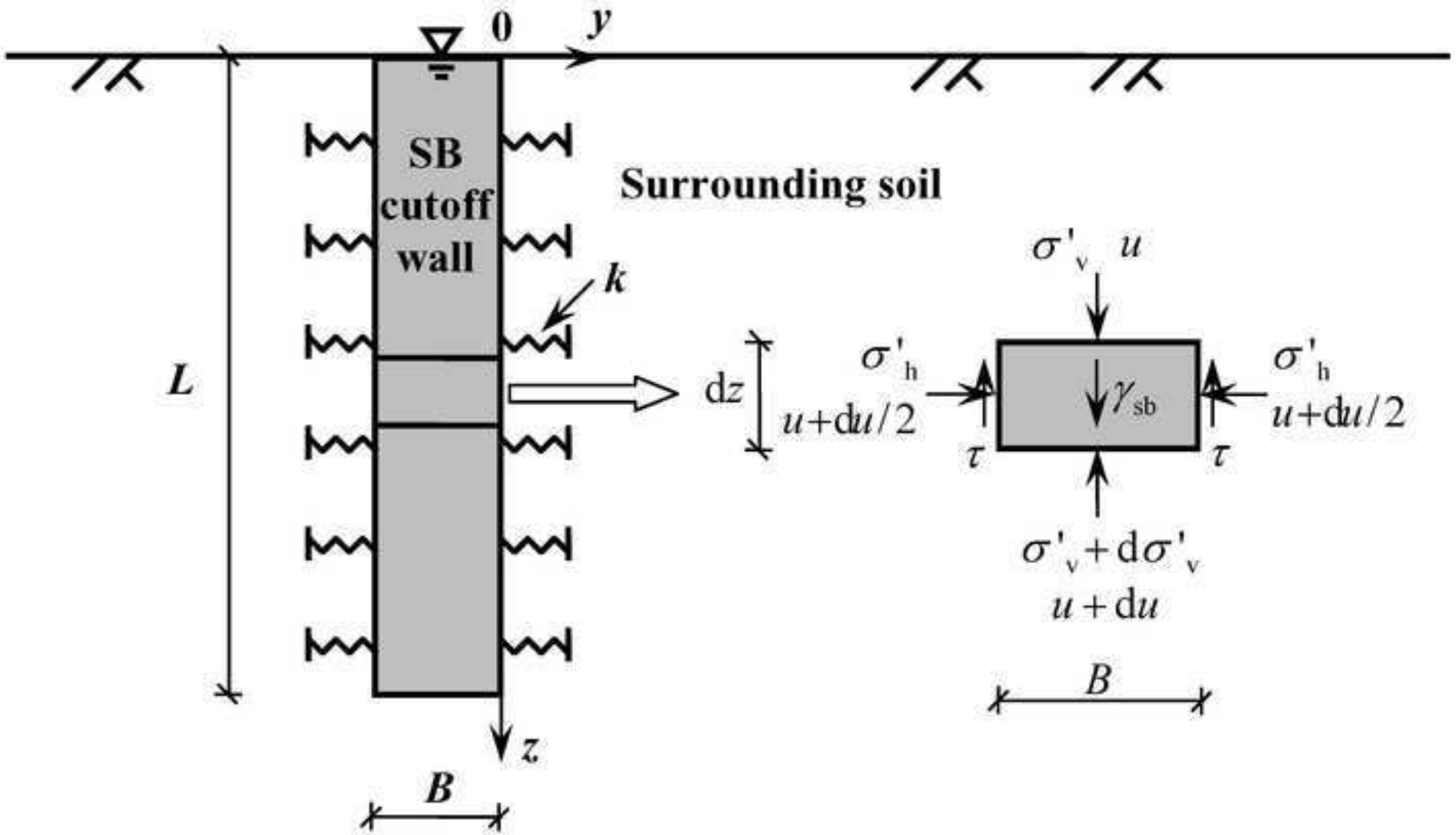
0
y
SB
cutoff
wall
Surrounding soil
k
L
dz
u+du/2
σ'v u
σ'h
σ'h
γsb
τ
τ
u+du/2
σ'v+dσ'v
u+du
B
z
B

Figure 2

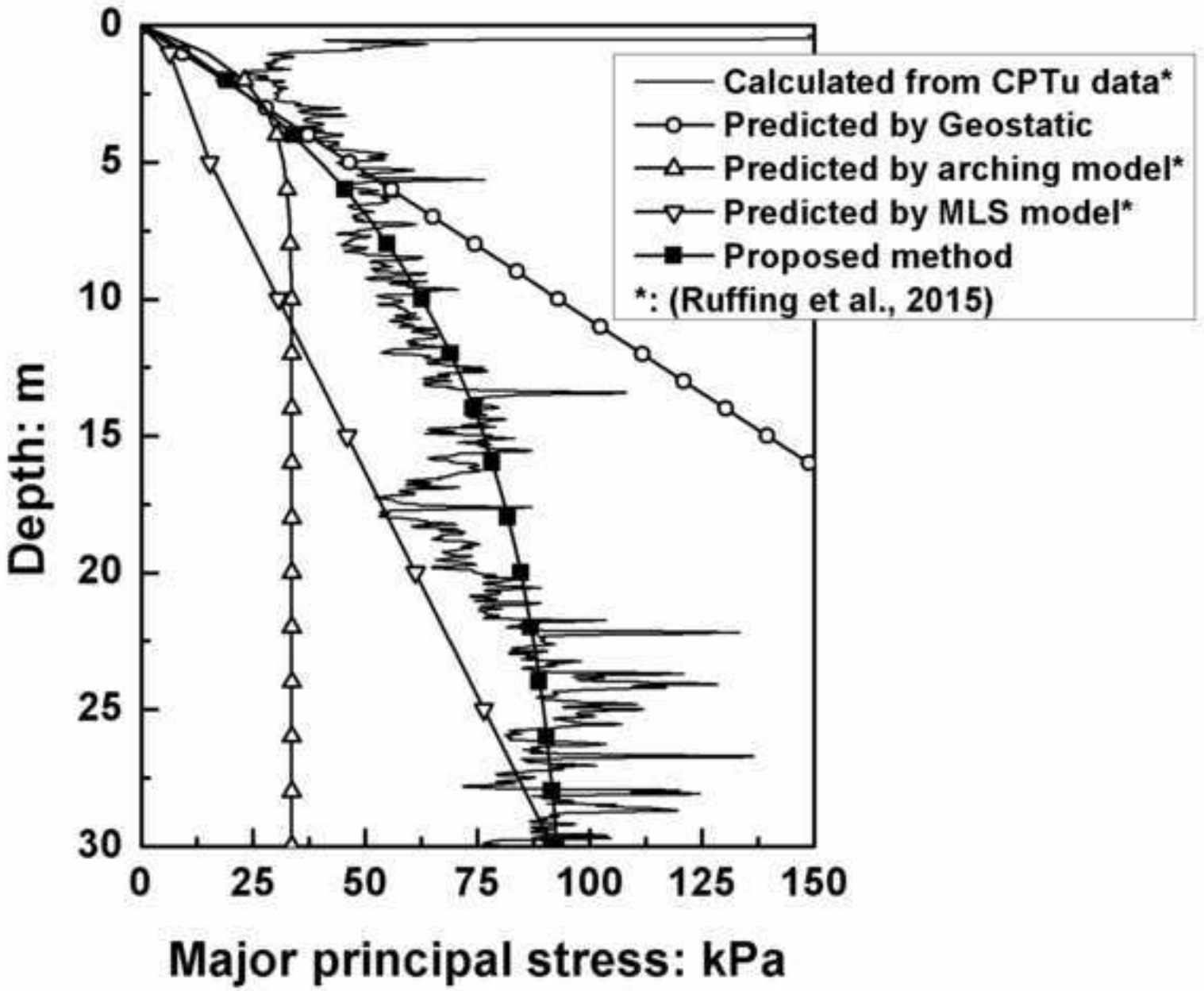
Calculated from CPTu data*
Predicted by Geostatic
Predicted by arching model*
Predicted by MLS model*
Proposed method
*: (Ruffing et al., 2015)
Depth: m
0
5
10
15
20
25
30
0
25
50
75
100
125
150
Major principal stress: kPa

Figure 3

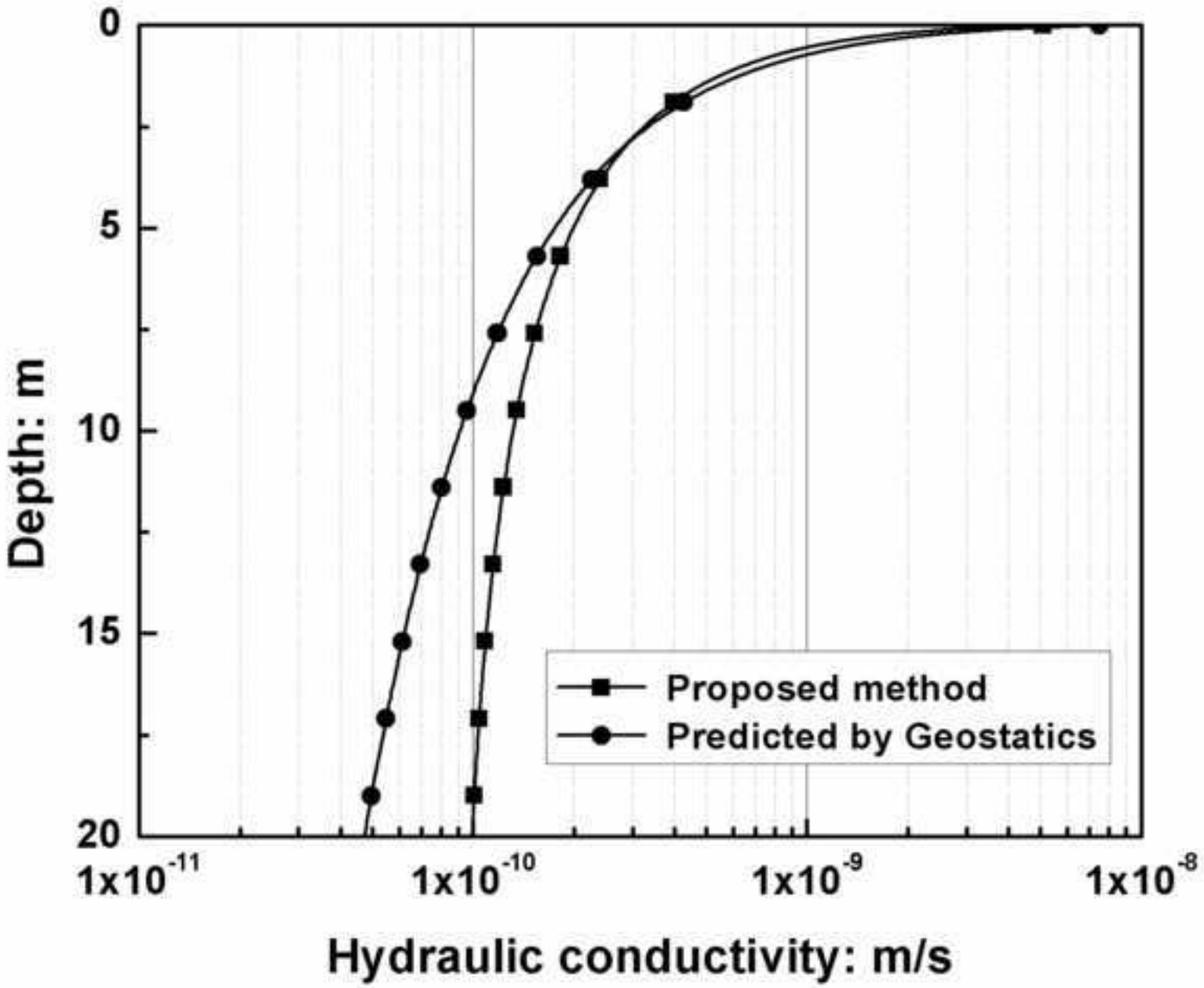
0
5
10
15
20
Depth: m
1x10-11
1x10-10
1x10-9
1x10-8
Hydraulic conductivity: m/s
Proposed method
Predicted by Geostatics

Figure 4(a)

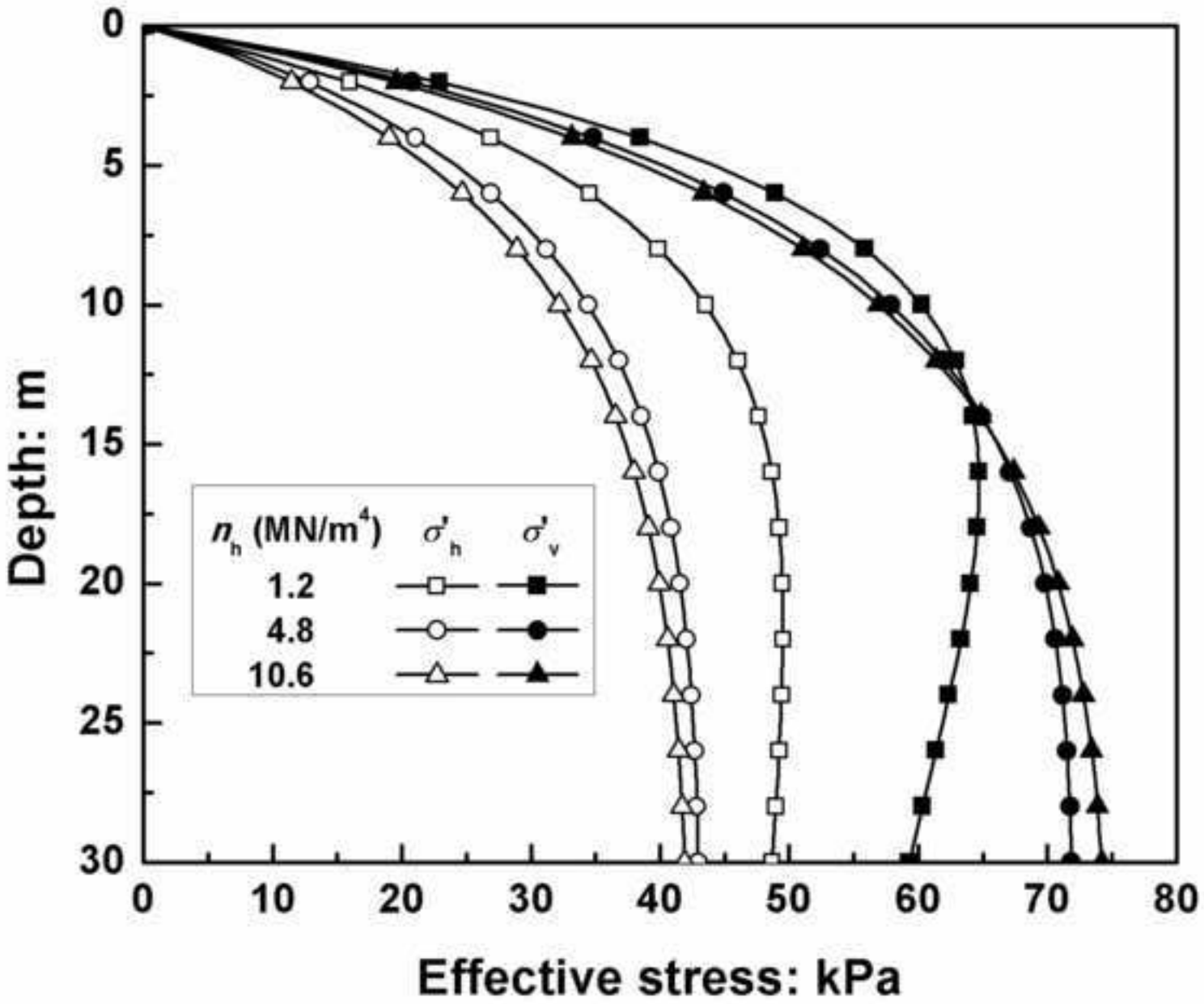
Depth: m
Effective stress: kPa
0
5
10
15
20
25
30
0
10
20
30
40
50
60
70
80
n_h (MN/m^4)
σ'_h
σ'_v
1.2
4.8
10.6

Figure 4(b)

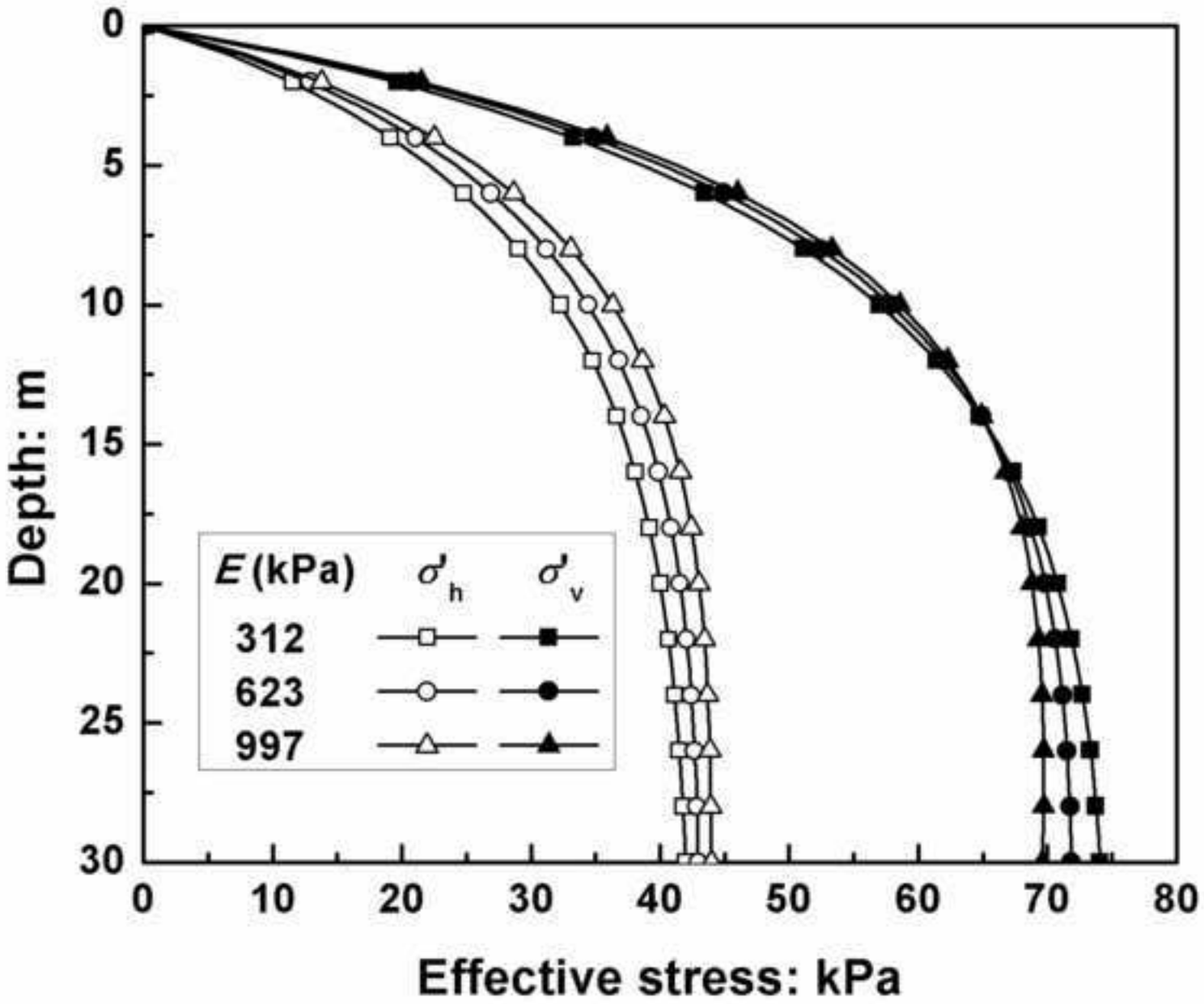
Depth: m
0
5
10
15
20
25
30
0
10
20
30
40
50
60
70
80
Effective stress: kPa
E (kPa)
σ'h
σ'v
312
623
997

Figure 4(c)

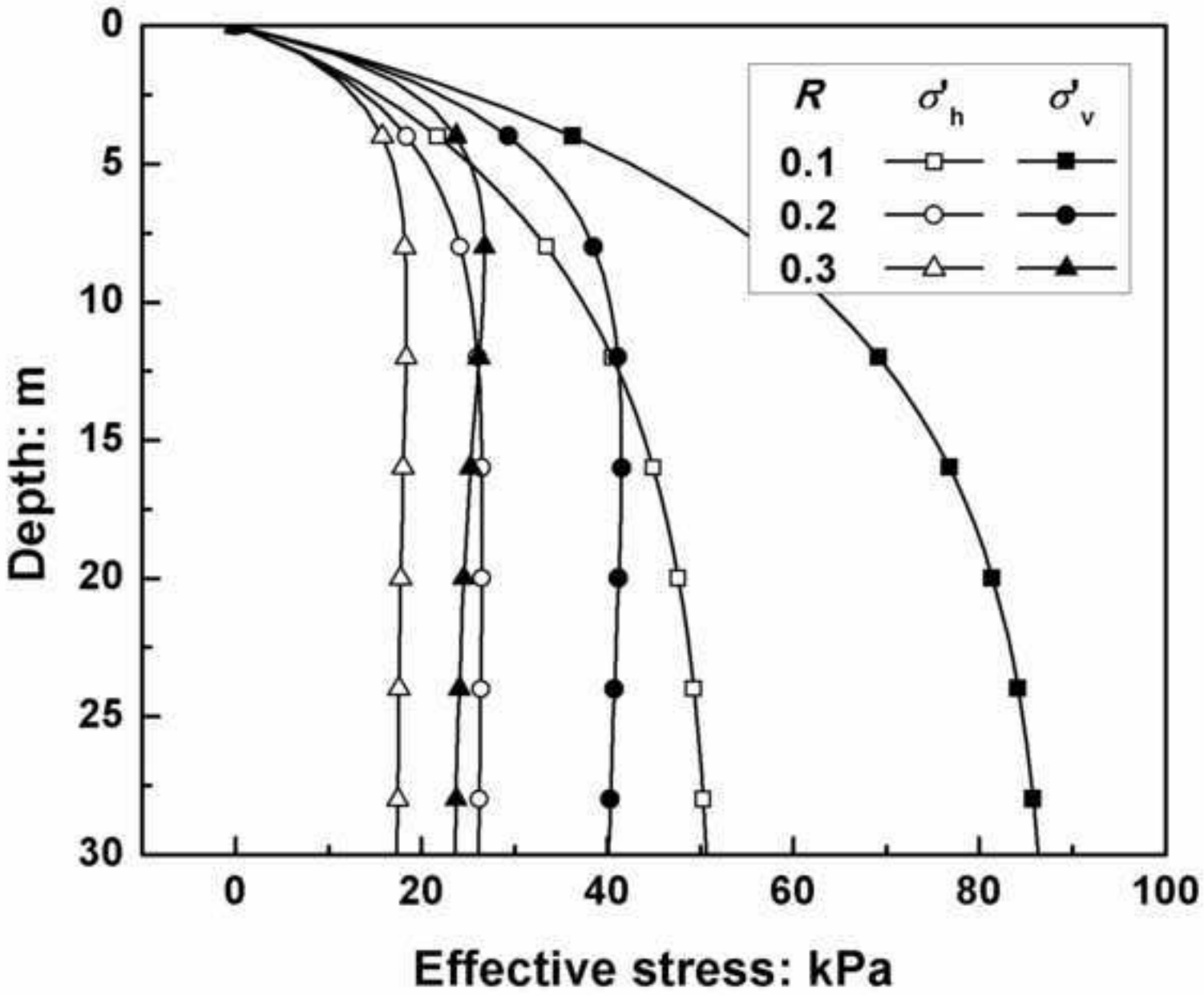
0
5
10
15
20
25
30
Depth: m
0
20
40
60
80
100
Effective stress: kPa
R
σ'h
σ'v
0.1
0.2
0.3

Figure 5

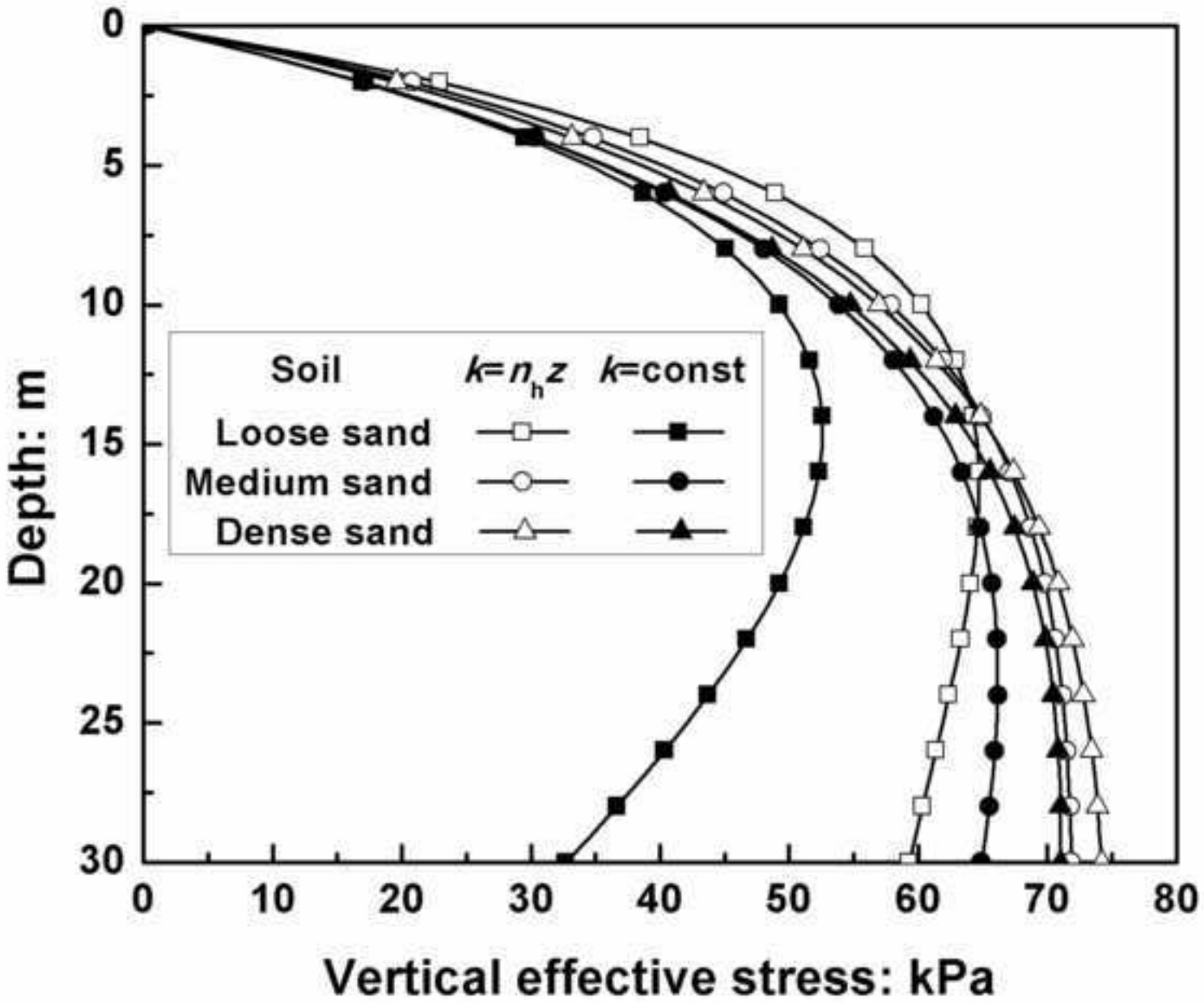
Depth: m
0
5
10
15
20
25
30
0
10
20
30
40
50
60
70
80
Vertical effective stress: kPa
Soil
k=n_h z
k=const
Loose sand
Medium sand
Dense sand